

# Nanoscale

Accepted Manuscript



This is an *Accepted Manuscript*, which has been through the Royal Society of Chemistry peer review process and has been accepted for publication.

*Accepted Manuscripts* are published online shortly after acceptance, before technical editing, formatting and proof reading. Using this free service, authors can make their results available to the community, in citable form, before we publish the edited article. We will replace this *Accepted Manuscript* with the edited and formatted *Advance Article* as soon as it is available.

You can find more information about *Accepted Manuscripts* in the [Information for Authors](#).

Please note that technical editing may introduce minor changes to the text and/or graphics, which may alter content. The journal's standard [Terms & Conditions](#) and the [Ethical guidelines](#) still apply. In no event shall the Royal Society of Chemistry be held responsible for any errors or omissions in this *Accepted Manuscript* or any consequences arising from the use of any information it contains.

# Enzymatic Etching of Gold Nanorods by Horseradish Peroxidase and Application to Blood Glucose Detection

Laura Saa<sup>a,§</sup>, Marc Coronado-Puchau<sup>a,§</sup>, Valeri Pavlov<sup>a,\*</sup>, and Luis M. Liz-Marzán<sup>a,b,\*</sup>

<sup>a</sup> *CIC biomaGUNE, Paseo de Miramón 182, 20009 Donostia - San Sebastián, Spain*

<sup>b</sup> *Ikerbasque, Basque Foundation for Science, 48011 Bilbao, Spain*

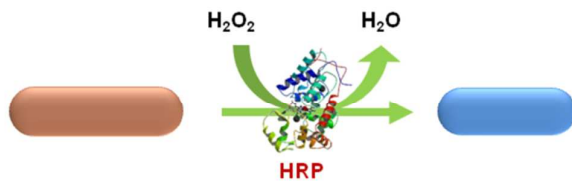
<sup>§</sup> These authors contributed equally

\* Corresponding authors: vpavlov@cicbiomagune.es; lizmarzan@cicbiomagune.es

## ABSTRACT

Gold nanorods (AuNR) have become one of the most used nanostructures for biosensing and imaging applications due to their plasmon-related optical response, which is highly sensitive toward minute changes in AuNR aspect ratio. In this context, H<sub>2</sub>O<sub>2</sub> has been used to trigger the chemical etching of AuNRs, thereby inducing a decrease of their aspect ratio. However, special conditions and relatively high concentrations of H<sub>2</sub>O<sub>2</sub> are usually required, preventing the applicability of the system for biodetection purposes. To overcome this limitation we have introduced a biocatalytic species, the enzyme horseradish peroxidase (HRP) that is able to induce a gradual oxidation of AuNRs in the presence of trace concentrations of H<sub>2</sub>O<sub>2</sub>. Interestingly, the presence of halide ions has also been found to be essential for this process. As a consequence, other enzymatic reactions, such as those catalyzed by glucose oxidase, can be easily coupled to HRP activity, allowing the detection of different amounts of glucose. On the basis of these findings, we developed a highly sensitive and simple colorimetric assay that can be read out by the bare eye and allows the detection of physiological glucose concentrations in human serum.

Table of Contents entry:



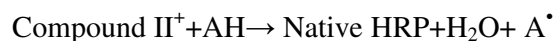
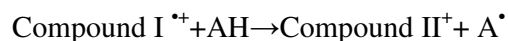
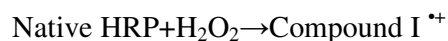
Enzymatic oxidation of gold nanorods by the enzymatic activity of horseradish peroxidase

## 1. INTRODUCTION

Noble metal nanoparticles exhibit fascinating physical properties that are extremely sensitive to their size, shape and composition.<sup>1</sup> Gold nanoparticles in particular display strong localized surface plasmon resonances (LSPRs) within the visible or near-IR, which make them very useful for a wide range of applications. In this context, gold nanoparticles have been broadly applied for the development of various colorimetric sensors.<sup>2-4</sup> Among other shapes, gold nanorods (AuNRs) have gained increased attention in biosensing because their longitudinal LSPR band is highly sensitive to minute changes in the AuNR aspect ratio,<sup>5, 6</sup> so that the optical response can be tuned in a wide wavelength range by simply changing the aspect ratio. Shortening of gold nanorods,<sup>7</sup> transverse overgrowth,<sup>8</sup> and lateral etching<sup>9</sup> are a few examples of post-synthetic morphological modification of AuNRs.

One strategy for tuning the aspect ratio of AuNRs, and consequently their optical properties, is partial oxidation under mild conditions. For example, it has been shown that AuNRs etching by H<sub>2</sub>O<sub>2</sub> takes place under acidic conditions.<sup>10</sup> However, high concentrations of oxidizing agents and high temperature are usually required, thereby preventing the applicability of this system for biodetection purposes. In order to overcome this issue, when lower H<sub>2</sub>O<sub>2</sub> concentrations are used, catalytic species should be introduced to trigger the chemical etching of the AuNRs. Most of these species are metal ions such as ferric<sup>9, 11</sup> or copper ions.<sup>12</sup> Still, the low specificity of these ions together with the relatively high concentrations of H<sub>2</sub>O<sub>2</sub> represent an important limitation toward biodetection. Therefore, the introduction of biocatalytic species could significantly improve the efficiency and biocompatibility of the system, thereby opening new possibilities in biosensing using AuNRs.

One of these biological species is the enzyme horseradish peroxidase (HRP).<sup>13</sup> HRP is composed of a glycoprotein containing 308 amino acid residues and the active center hemin,<sup>14</sup> and can catalyze the oxidation of various electron donor substrates including 2,3-dimethoxyphenol, guaiacol, 5-amino-2,3-dihydro-1,4-phthalazinedione (luminol), 2,2'-azino-bis(3-ethylbenzothiazoline-6-sulfonate) (ABTS), and 3,3',5,5'-tetramethylbenzidine (TMB). The catalytic reaction is a three-step cyclic process. First, hemin complexed with the protein shell is oxidized by hydrogen peroxide forming a double covalent bond between iron in hemin and an oxygen atom from H<sub>2</sub>O<sub>2</sub>, to yield Compound I, which is a hemin derivative bearing an oxoferryl group (Fe<sup>IV</sup>=O). This derivative can oxidize the first reducing substrate molecule through single-electron transfer, discharging the  $\pi$ -cation radical. The resulting intermediate still containing an oxoferryl group is called Compound II. A second substrate molecule reduces Compound II through a single-electron transfer to the native ferric hemin containing Fe<sup>III</sup>. During this transformation, oxygen is released from an oxoferryl group when it accepts two protons forming a water molecule. During the reaction cycle of HRP two substrate molecules (AH) turn into two free radicals (A $\cdot$ ) according to the following equations.<sup>15</sup>



HRP has been extensively used in biology and biotechnology for its unique characteristics, low cost and ability to form coupled enzyme assays.<sup>15, 16</sup> We present in this paper the effect of HRP on the enzymatic anisotropic etching of AuNRs when trace concentrations of H<sub>2</sub>O<sub>2</sub> are present. Since HRP can be easily coupled to other enzymes, we coupled HRP to glucose oxidase (GOx), generating H<sub>2</sub>O<sub>2</sub> from glucose oxidation,

which may provide a novel method for glucose detection. In some recent works, the generation of  $\text{H}_2\text{O}_2$  by GOx has been employed for the oxidation of metal nanoparticles, enabling the development of colorimetric glucose biosensors.<sup>17,18</sup> However, these experiments are usually time-consuming and costly. As a consequence, the introduction of HRP, an enzyme that presents very fast reaction kinetics and substrate turnover rates may be of interest for plasmonic assisted biosensing. Therefore, in this work we developed a simple and fast colorimetric assay for the detection of glucose, which can be directly read out by the naked eye.

## 2. RESULTS AND DISCUSSION

### 2.1. Enzymatic etching of AuNRs by HRP

The effect of the enzymatic activity of HRP on the etching of AuNRs was first investigated in the presence of cetyltrimethylammonium bromide. Different concentrations of  $\text{H}_2\text{O}_2$  were added to an AuNR solution  $[\text{Au}^0]=0.12$  mM containing HRP (1.5  $\mu\text{M}$ ) and citrate buffer (20 mM, pH=4.0). As shown in **Figure 1**, in the presence of  $\text{H}_2\text{O}_2$  and HRP, oxidation of the AuNRs occurs with the subsequent decrease in AuNR size (**Figure 1A**). Statistical analysis from transmission electron microscopy (TEM) images was used to analyze the length and thickness of the AuNRs before and after oxidation. Initially, the AuNRs were about 60 nm long and 15 nm thick. However, upon addition of  $\text{H}_2\text{O}_2$  the NR length was gradually reduced while the thickness remained constant (**Figure 1B**). When a sufficient amount of  $\text{H}_2\text{O}_2$  was added, the rod-like shape was lost and spherical particles were obtained. It is important to note at this point that the oxidation was negligible in the absence of HRP, even at  $\text{H}_2\text{O}_2$  concentrations as high as 100  $\mu\text{M}$ . The TEM results, together with the observed

changes in the LSPR band of the AuNRs after addition of different amounts of HRP confirm that the enzymatic activity of HRP is essential for the efficient etching of AuNRs under these conditions (see ESI, Figure S1). Although the precise mechanism underlying this process is beyond the aim of this study, we postulate that in the presence of  $\text{H}_2\text{O}_2$ , the HRP heme group may generate a hydroxyl radical with a stronger oxidizing ability than  $\text{H}_2\text{O}_2$  itself, hence facilitating the above described oxidation reaction within a time scale of minutes. The observed anisotropic oxidation of the AuNRs is clearly reflected in a blue shift and a decrease in the intensity of the longitudinal LSPR band, initially centered at 850 nm, which gradually increases with the supply of  $\text{H}_2\text{O}_2$ . Therefore, the amount of  $\text{H}_2\text{O}_2$  can be correlated to the observed longitudinal LSPR shift, for which a linear correlation was found in the  $\text{H}_2\text{O}_2$  concentration range between 0 and 60  $\mu\text{M}$  (**Figure 1D**). Such an etching process eventually leads to formation of spherical nanoparticles and even to complete dissolution.

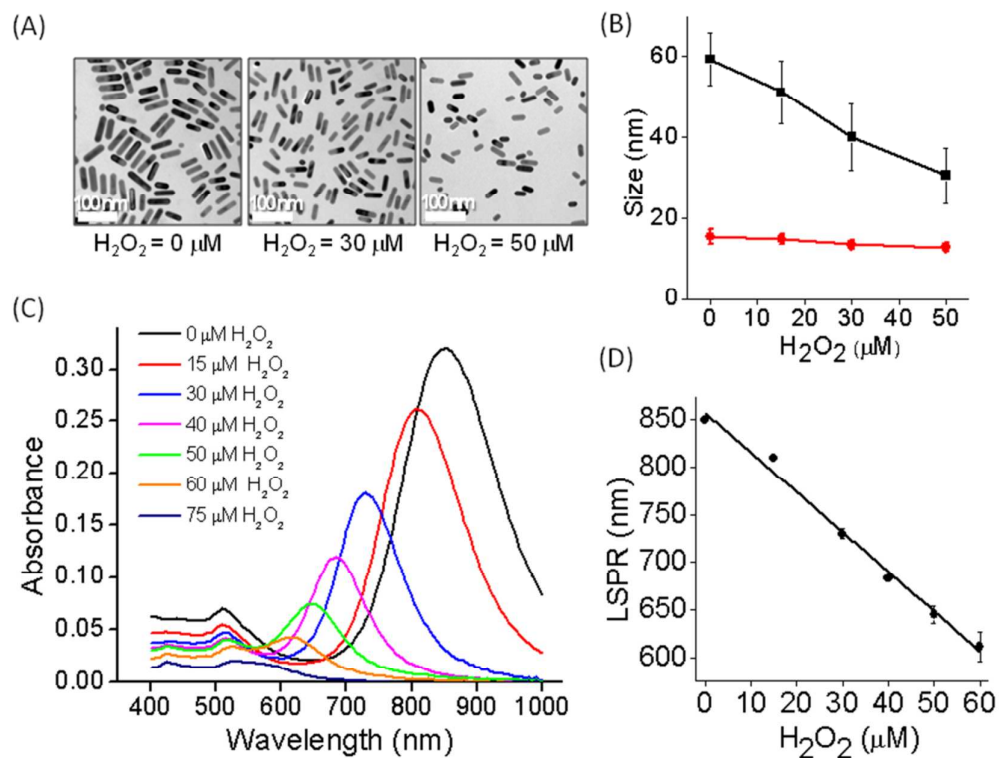


**Figure 1.** Enzymatic etching of AuNR by HRP (A) TEM images of the initial AuNRs and after addition of different H<sub>2</sub>O<sub>2</sub> concentrations. (B) Length (black squares) and width (red circles) of the AuNRs as a function of H<sub>2</sub>O<sub>2</sub> concentration. (C) Vis-NIR spectra after the incubation (15 min) of AuNRs with HRP (1.5 μM) and different concentrations of H<sub>2</sub>O<sub>2</sub> (D) LSPR shift as a function of H<sub>2</sub>O<sub>2</sub> concentration. Scale bars are the same for all images and represent 100 nm.

## 2.2. Role of halides on AuNRs etching

For certain applications, purification of the AuNRs and removal of excess surfactant may be required. However, we found that when the AuNRs were washed (twice) to remove excess CTAB, the oxidation reaction did not proceed. Since this was likely to be related to the removal of halide counterions, we tested the effect of adding bromide after purification. Thus, different concentrations of a bromide salt (NaBr) were added to the enzymatic solution to achieve a controlled concentration of anions. Indeed, the increase of [Br<sup>-</sup>] was found to enhance AuNR etching (**Figure 2**). In other words, as



more bromide was added to a solution containing  $\text{H}_2\text{O}_2$  (50  $\mu\text{M}$ ) and HRP (1  $\mu\text{M}$ ), the length of the AuNRs decreased accordingly. Again, when no bromide was added the AuNRs were stable and no etching was observed. This result is in agreement with previous work in which addition of  $\text{HAuCl}_4$  in the presence of CTAB led to rapid oxidation of AuNRs, although in this case the complexation of Au(III) ions with CTAB also played an important role.<sup>19</sup> Replacing bromide for other halides such as chloride and iodide was found to lead to different AuNR oxidation rates. Thus, in the presence of  $\text{Cl}^-$  the oxidation is very slow and the longitudinal LSPR band does not shift upon addition of NaCl. In contrast, addition of NaI leads to efficient oxidation of the NRs, resulting in complete damping of the longitudinal band with iodide concentrations as low as 20 mM (**Figure S2**). The origin of such a difference arises from the redox potential of the various gold halides. In the three cases considered herein,  $\text{Cl}^-$ ,  $\text{Br}^-$ , and  $\text{I}^-$ , the formation of the halide is favored. Oxidation of the Au NRs by either  $\text{H}_2\text{O}_2$  or hydroxyl radicals occurs spontaneously in all three cases. On the other hand, according to the reduction potential of the gold halides, the oxidation trend follows the order:  $\text{AuClx}^- < \text{AuBrx}^- < \text{AuIx}^-$ , since the reduction potential for the Au halides follows the reverse order (see **Table S1**, S.I.). In conclusion, by forming a Au halide, the anions favor the oxidation of the Au nanorods. The extent of this oxidation depends upon the redox potential of the Au halides, as predicted thermodynamically and observed experimentally.

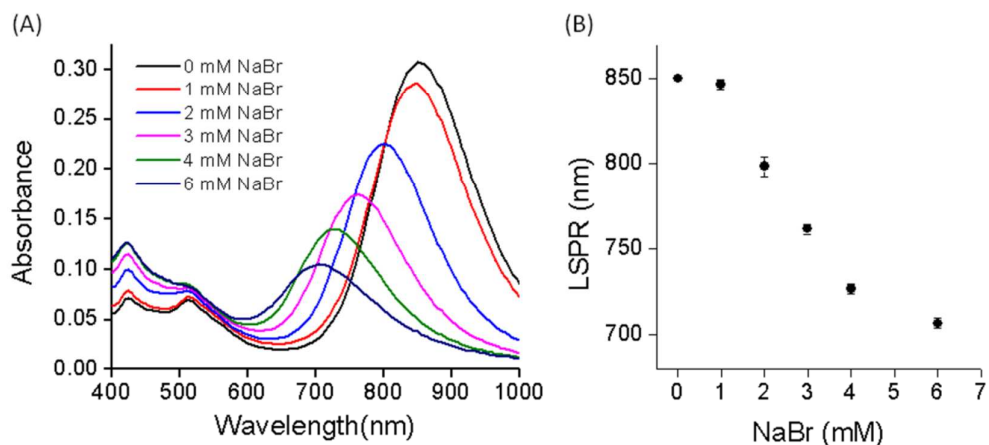


**Figure 2.** Effect of bromide on the enzymatic etching of AuNRs. (A) Vis-NIR spectra of AuNRs after incubation in the presence of HRP (1  $\mu\text{M}$ ),  $\text{H}_2\text{O}_2$  (50  $\mu\text{M}$ ) and different concentrations of NaBr. (B) Shift of the LSPR maxima as a function of NaBr concentration.

In view of these findings we further investigated the oxidation of gold nanoparticles with different shapes and capping molecules. Spherical citrate gold nanoparticles (AuNS@citrate) and polyvinylpyrrolidone coated gold nanostars (AuNs@PVP) were enzymatically oxidized in the presence of 1  $\mu\text{M}$  HRP, 25 mM NaBr and different concentrations of  $\text{H}_2\text{O}_2$ . As in the case of AuNRs, a decrease of the plasmon bands was observed, together with a blue shift in the case of AuNs@PVP (**Figure S3**). These results are consistent with the changes in the size and shape previously observed for AuNRs. Thus, in a more general context, we can conclude that the presence of halides in solution is required for the enzymatic oxidation of gold nanoparticles, regardless of the capping agent.

### 2.3. Plasmon-assisted glucose biosensing

We have seen in the previous section that HRP can oxidize gold nanoparticles in the presence of  $\text{H}_2\text{O}_2$  and a halide acting as gold complexing agent. This feature can be exploited to develop a colorimetric method for the detection of glucose, by coupling the enzymatic activity of glucose oxidase (GOx) to HRP activity (**Figure 3A**). We postulated that AuNRs etching would serve as a reporter for any enzymatic reaction coupled to the HRP reaction. However, we found that this assessment is only true when the pH of the reaction medium is acidic (data not shown). Therefore, GOx was selected for this purpose since this enzyme has been shown to remain active under acidic pH conditions (The present study was performed in citrate buffer, pH=4.0). GOx catalyses the oxidation of glucose, generating  $\text{H}_2\text{O}_2$  as a reaction product. The addition of aqueous solutions with different glucose concentrations to a solution containing HRP, GOx and AuNRs leads to a gradual blue shift of the longitudinal LSPR, which can be easily monitored by Vis-NIR spectroscopy (**Figure 3B**). A linear correlation between the amount of glucose added to the solution and the shift of the AuNRs longitudinal band was clearly observed in the concentration range from 0 to 250  $\mu\text{M}$ . This provides a highly sensitive method for the detection of glucose (with a detection limit of 10  $\mu\text{M}$ ). This limit of detection was obtained considering 3 standard deviations above the mean background (**Figure 3C**). Control experiments (**Figure S5, ESI**) demonstrate that no oxidation takes place in the absence of HRP.

Upon optimization of this enzymatic coupled activity, human serum of unknown glucose concentration was analyzed to demonstrate the practical application of this plasmon-assisted biosensor. Note that the usual concentration of glucose in human blood lies within the mM range, while the high sensitivity of this method allows us to carry out detection in the  $\mu\text{M}$  range. Hence, human serum samples were diluted 50-fold prior to the analysis. The concentration of glucose in the human samples was quantified

by the method of the standard addition. Human serum was added to standard solutions containing different concentrations of glucose from 0 to 80  $\mu\text{M}$ . The experimental data were plotted as concentration of added glucose vs. LSPR shift. As shown in **Figure 3D**, a linear regression was performed to calculate the position of the X-intercept of the calibration line, which showed the concentration of glucose in the diluted real sample. Taking the dilution factor into consideration, a glucose concentration in the human plasma of 5.31 mM was determined. This concentration is within the physiological range, thus demonstrating that this method is valid for the detection of glucose in human blood. Note that a standard colorimetric procedure yielded a value of 5.11 mM for the same human serum sample (data not shown). A similar plasmonic glucose biosensor has been reported by Liu et al.,<sup>18</sup> based on AuNRs etching mediated by the Fenton reagent  $\text{Fe}^{2+}$ -EDTA. The advantage of using HRP instead of the Fenton reagent for this particular application is that AuNR oxidation is much faster and sensitive (see a comparison in **Figure 4S**). In the work reported in ref. [18], comparatively high concentrations of  $\text{H}_2\text{O}_2$  were required to oxidize the AuNRs, even in presence of CTAB.

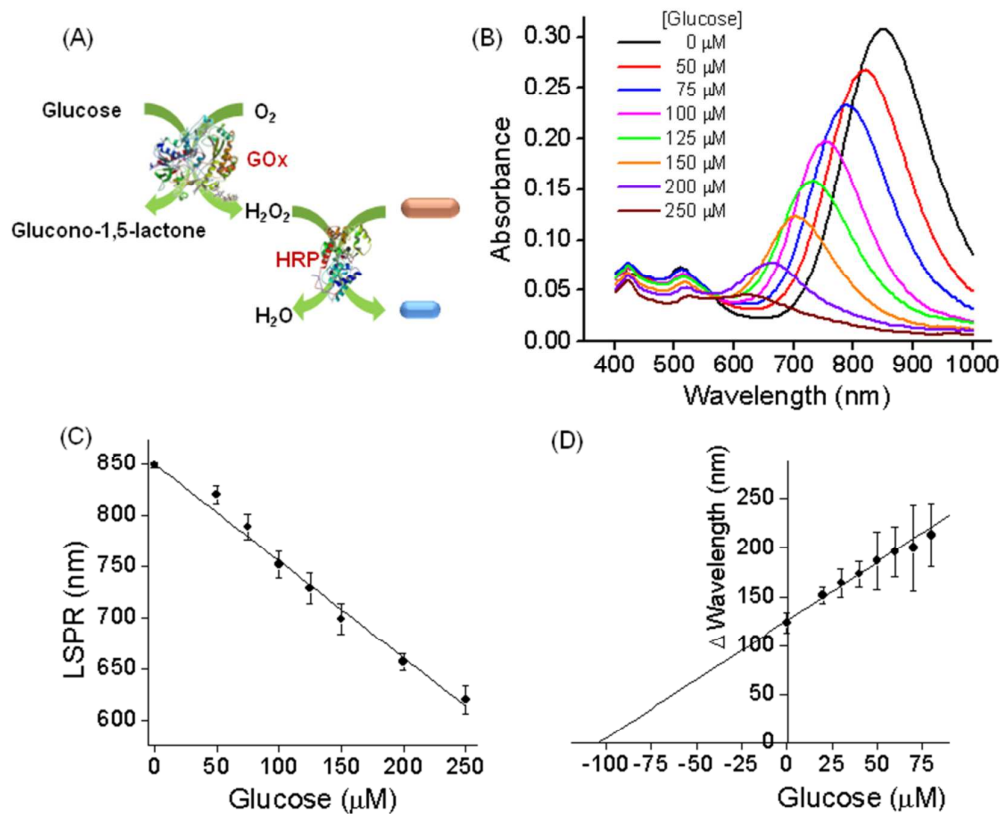


**Figure 3.** Enzymatic etching of AuNRs for glucose biosensing. (A) Schematic view of the enzymatic etching of AuNRs by coupled activity of GOx and HRP. (B) Vis-NIR spectra of AuNRs solution before and after incubation in the presence of HRP (1.5 μM), GOx (50 nM) and different concentrations of glucose as indicated. (C) LSPR shift as a function of glucose concentration. (D) Quantification of glucose concentration in human serum via the method of standard addition.

Practical application of this colorimetric biosensing method may require that non-trained users can easily perform the sensing assay. For this purpose, we carried out a simplified implementation of the sensor, based on silica gels prepared by a simple sol-gel preparation,<sup>20</sup> in which AuNRs were embedded in the presence of HRP 3.2 μM, GOx 140 nM and NaBr 25 mM. Addition of a glucose solution on the so formed composite silica monolith leads to a color change from pink to yellow, reflecting the oxidation of the AuNRs (**Figure 4**). It is important to note that the thickness of the silica gel is of relevance for this process. The slow diffusion of the glucose solution through

the gel triggers the observation of a range of colors with time, from yellow through pink, depending on the oxidation stage of the AuNRs (**Figure 4A**). The color of the AuNRs in the gel, prior to glucose addition, is light pink whereas in the presence of glucose AuNRs etching leads to a color change into blue, and eventually into yellow due to complete oxidation from  $\text{Au}^0$  to  $\text{Au(III)}$ . The reaction conditions and the thickness of the gel were thus optimized to develop a simple device for the detection of glucose with the naked eye. As displayed in **Figure 4**, addition of a 5 mM glucose solution was sufficient to change the color from pink to yellow. This concentration is close to the usual glucose level in human blood (ca. 5.5 mM).

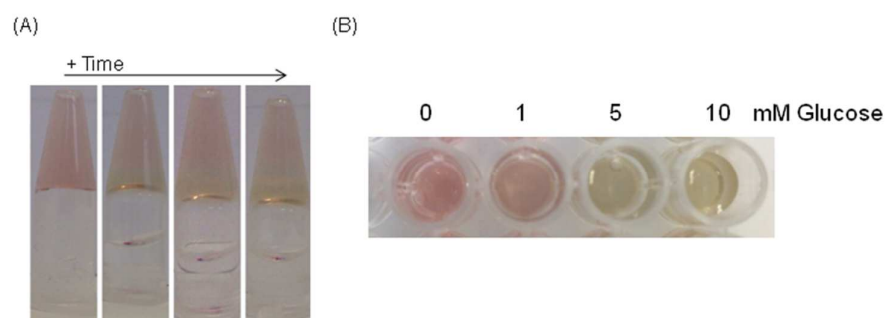


**Figure 4.** Glucose detection in silica gel/enzymes/AuNRs composites. (A) Kinetics of AuNR oxidation in a silica gel within an eppendorf tube. Note that the increase of the AuNR oxidation with time leads to an increase of the yellow band. (B) Colorimetric detection of glucose in thin silica gels loaded on well plates.

## CONCLUSIONS

We have demonstrated that the enzymatic activity of horseradish peroxidase can induce the gradual oxidation of AuNRs and other gold nanoparticles, in the presence of halide ions as gold complexing agents. As a consequence of AuNR shortening, the position of

the longitudinal LSPR band of the AuNRs can be used to determine the concentration of  $\text{H}_2\text{O}_2$  in solution. On the basis of this process, we developed a simple colorimetric assay for the detection of glucose that allows detection of physiological glucose concentrations. The use of HRP in this reaction represents a significant improvement with respect to previously reported plasmonic assisted glucose biosensors.

### 3. EXPERIMENTAL SECTION

**3.1. Materials.**  $\text{HAuCl}_4 \cdot 3\text{H}_2\text{O}$  (99%), cetyltrimethylammonium bromide (CTAB), sodium borohydride ( $\text{NaBH}_4$ ), silver nitrate ( $\text{AgNO}_3$ ), glucose oxidase type VII from *aspergillus niger*, horseradish peroxidase type VI and other chemicals were supplied by Sigma-Aldrich. Milli-Q  $\text{H}_2\text{O}$  (Millipore, Billerica, MA, USA) was used as solvent. All chemicals were used as received from the supplier. Absorbance measurements were performed in a Varioskan Flash microplate reader (Thermo Scientific) using 96-microwell plates. The UV-Vis absorbance spectra were scanned from 400 to 1000 nm at 30 °C.

**3.2. Gold nanorod synthesis:** AuNRs were prepared by seed mediated growth<sup>6,21</sup>. The seeds were made by adding a freshly prepared  $\text{NaBH}_4$  solution (0.3 mL, 0.01 M) to another solution containing  $\text{HAuCl}_4$  (0.025 mL, 0.05 M) and CTAB (4.7 mL, 0.1 M). The growth solution was prepared by adding ascorbic acid (0.08 mL, 0.1 M) to a solution containing  $\text{HAuCl}_4$  (0.1 mL, 0.05 M),  $\text{AgNO}_3$  (0.12 mL, 0.01 M), HCl (0.19 mL, 1 M), and CTAB (10 mL, 0.1 M).

**3.3. HRP assay:** Varying concentrations of  $\text{H}_2\text{O}_2$  were added to a solution containing AuNRs ( $[\text{Au}^0]=0.12$  mM), CTAB 5 mM, HRP (1.5  $\mu\text{M}$ ) and citrate buffer 20 mM pH

4.0, in a final volume of 100  $\mu$ L. The absorbance spectra of the resulting mixtures were recorded after 15 min.

**3.4. GOx assay:** Varying concentrations of glucose were added to a solution containing AuNRs ( $[Au^0]=0.12$  mM), CTAB 5 mM, HRP (1.5  $\mu$ M), GOx (50 nM) and citrate buffer 20 mM, pH 4.0, in a final volume of 100  $\mu$ L. The absorbance spectra of the resulting mixtures were recorded after 15 min.

**3.5. Effect of the halides.** In order to remove excess CTAB, AuNRs were washed by centrifugation at 7000 rpm for 20 min. The supernatant was discarded and the precipitate was redispersed in water until reaching the initial volume. Afterwards, the washed AuNRs were used in the HRP assay as described above.

**3.6. Quantification of glucose in human serum:** commercial human serum (Sigma-Aldrich) was centrifuged on Amicon Ultra filter with a 3,000 molecular weight cutoff. After filtering, serum was spiked with different concentrations of glucose and the glucose concentration of the mixtures was determined as described above. The dilution factor of serum in the assay was 1:50.

**3.7. Preparation of silica gel/enzymes/AuNRs composites.** Sol-gel based silica matrices were prepared according to Luckham and Brennan.<sup>20</sup> Briefly, 10 mL of H<sub>2</sub>O were mixed with 2.9 g of sodium silicate solution followed by addition of 5 g of Dowex cation exchange resin to replace Na<sup>+</sup> with H<sup>+</sup>. The mixture was stirred until reaching a final pH = 4 and filtrated to remove the resin. This silicate precursor was then mixed in a 1:1 ratio with a solution containing AuNRs 0.78 mM, HRP 3.4  $\mu$ M, GOx, 0.28  $\mu$ M,



NaBr 50 mM in citrate buffer 0.2 M pH 4.0. The mixtures were then allowed to cure in microplate wells for 48 h at 4 °C prior to use. Samples of 100 µL containing different concentrations of glucose were added to the silica gel matrix, and the change in the color of the silica gels was followed by the naked eye.

### Acknowledgements

L.S. and V.P. acknowledge financial support from the Spanish Ministry of Economy and Competitiveness (project BIO2011-26365). M.C.-P. acknowledges an FPU Scholarship from the Spanish Ministry of Education, Culture and Sports. L.M.L.-M. acknowledge financial support from the European Research Council (ERC Advanced Grant #267867 Plasmaquo).

### References

1. K. L. Kelly, E. Coronado, L. L. Zhao and G. C. Schatz, *J. Phys. Chem. B*, 2002, **107**, 668-677.
2. L. Rodriguez-Lorenzo, R. de la Rica, R. A. Alvarez-Puebla, L. M. Liz-Marzan and M. M. Stevens, *Nat. Mater.*, 2012, **11**, 604-607.
3. L. Guo, Y. Xu, A. R. Ferhan, G. Chen and D.-H. Kim, *J. Am. Chem. Soc.*, 2013, **135**, 12338-12345.
4. Y. Xianyu, J. Sun, Y. Li, Y. Tian, Z. Wang and X. Jiang, *Nanoscale*, 2013, **5**, 6303-6306.
5. M. Coronado-Puchau, L. Saa, M. Grzelczak, V. Pavlov and L. M. Liz-Marzan, *Nano Today*, 2013, **8**, 461-468.
6. J. Perez-Juste, I. Pastoriza-Santos, L. M. Liz-Marzan and P. Mulvaney, *Coord. Chem. Rev.*, 2005, **249**, 1870-1901.
7. C.-K. Tsung, X. Kou, Q. Shi, J. Zhang, M. H. Yeung, J. Wang and G. D. Stucky, *J. Am. Chem. Soc.*, 2006, **128**, 5352-5353.
8. X. Kou, S. Zhang, Z. Yang, C.-K. Tsung, G. D. Stucky, L. Sun, J. Wang and C. Yan, *J. Am. Chem. Soc.*, 2007, **129**, 6402-6404.
9. X. Guo, Q. Zhang, Y. Sun, Q. Zhao and J. Yang, *ACS Nano*, 2012, **6**, 1165-1175.
10. G. Chandrasekar, K. Mougin, H. Haidara, L. Vidal and E. Gnecco, *Appl. Surf. Sci.*, 2011, **257**, 4175-4179.
11. R. Zou, X. Guo, J. Yang, D. Li, F. Peng, L. Zhang, H. Wang and H. Yu, *CrystEngComm*, 2009, **11**, 2797-2803.
12. T. S. Sreerasad, A. K. Samal and T. Pradeep, *Langmuir*, 2007, **23**, 9463-9471.

13. J. Everse, K. E. Everse and M. B. Grisham, *Peroxidases in Chemistry and Biology, Volume II*, CRC Press, 1990.
14. K. G. Welinder, *FEBS Lett.*, 1976, **72**, 19-23.
15. A. M. Azevedo, V. C. Martins, D. M. Prazeres, V. Vojinovic, J. M. Cabral and L. P. Fonseca, *Biotechnol. Annu. Rev.*, 2003, **9**, 199-247.
16. N. C. Veitch, *Phytochemistry*, 2004, **65**, 249-259.
17. Y. Xia, J. Ye, K. Tan, J. Wang and G. Yang, *Anal. Chem.*, 2013, **85**, 6241-6247.
18. X. Liu, S. Zhang, P. Tan, J. Zhou, Y. Huang, Z. Nie and S. Yao, *Chem. Commun.*, 2013, **49**, 1856-1858.
19. J. Rodriguez-Fernandez, J. Perez-Juste, P. Mulvaney and L. M. Liz-Marzan, *J. Phys. Chem. B*, 2005, **109**, 14257-14261.
20. R. E. Luckham and J. D. Brennan, *Analyst*, 2010, **135**, 2028-2035.
21. B. Nikoobakht and M. A. El-Sayed, *Chem. Mater.*, 2003, **15**, 1957-1962.